Reactive and Functional Polymers 175 (2022) 105265

Contents lists available at ScienceDirect

Reactive and Functional Polymers

journal homepage: www.elsevier.com/locate/react

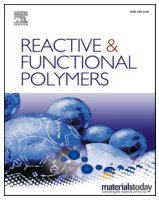

Perspective article

Chemical structures and compositions of peptide copolymer films affect their functional properties for cell adhesion and cell viability

Tienli Ma [a], Chiehming Tsai [a], Shyhchyang Luo [a], Weili Chen [b,c,d], Yuching Huang [e,*], Weifang Su [a,e,*]

[a] Department of Materials Science and Engineering, National Taiwan University, Taipei, Taiwan
[b] Department of Ophthalmology, National Taiwan University College of Medicine, Taipei, Taiwan
[c] Department of Ophthalmology, National Taiwan University Hospital, Taipei, Taiwan
[d] Advanced Ocular Surface and Corneal Nerve Regeneration Center, National Taiwan University Hospital, Taipei, Taiwan
[e] Department of Materials Engineering, Ming Chi University of Technology, New Taipei City, Taiwan

ARTICLE INFO

Keywords:
Peptide copolymer
Glutamate
Lysine
Structure
Composition
Interface
Cell culture

ABSTRACT

In this study we synthesized peptide copolymers containing benzyl glutamate (BG) moiety (to enhance cell viability) and lysine derivatives (to improve cell adhesion) for use in tissue engineering. We examined the effects of two lysine derivatives: N_ε-t-butyloxycarbonyl lysine (BOCL) and N_ε-carbobenzoxy lysine (CBZL). The cell behavior on the copolymer films was influenced by the functional characteristics of the copolymers, governed by their chemical structures and compositions. A BOC unit on the lysine side chain is bulkier than a CBZ unit, resulting in a rougher film surface displaying poorer adhesion. The film's hydrophilicity and cell adhesion properties were improved by increasing the CBZL content in the copolymers, due to the presence of the amide linkages of the CBZ units. The copolymer film prepared with an equal molar ratio of CBZL and BG exhibited the best cell performance, resulting from a balance in the copolymer's functional properties. The cell behavior on this film was further improved by partially hydrolyzing the copolymer to produce net positive charge, thereby increasing the hydrophilicity and cell recognition. These novel copolymers appear suitable for use as films for enhancing cell culturing during tissue engineering.

1. Introduction

Synthetic polypeptides are important biomimetic polymers for biomedical applications because their backbones have structures similar to those of proteins; they have outstanding biocompatibility, biodegradability, and chemical diversity; and they have the ability to form highly ordered structures [1–3]. Accordingly, they have found a diverse range of applications in, for example, drug delivery, gene delivery, tissue engineering, and antimicrobials [4–6]. These polypeptides can be synthesized through ring-opening polymerization (ROP) of *N*-carboxyanhydride (NCA) derivatives of amino acids in large quantities, with high molecular weights and narrow polydispersity indexes (PDI) [7].

Poly(glutamic acid) (PGA) and poly(benzyl glutamate) (PBG) are among the most widely investigated biomedical polypeptides because they have the ability to enhance cell viability [8,9]. For example, PGA core/shell nanofibrous scaffolds have been used for wound healing [10]; porous PBG scaffolds have been developed for bone tissue engineering [11]; and PBG monolayer have exhibited good biocompatibility toward L929 fibroblast cells [12]. PBG can not only increase cell activity but also stimulate neurogenesis and neurite outgrowth, because the glutamate component of PBG is a neurotransmitter capable of cell communication and differentiation to promote neurogenesis [13]. iPSC-derived retinal ganglion cell (RGC) progenitors and retinal organoids cultured on aligned PBG scaffolds have displayed superior and more efficient cell differentiation than those on cover slips, and they have shortened the differentiation processing time of RGC cells [14]. Pheochromocytoma (PC-12) cells on three-dimensional (3D) aligned PBG scaffolds have also displayed greater cell viability, differentiation, and proliferation than those on commercial polycaprolactone (PCL) [15]. Poly(L-lysine) (PLL) is another important water-soluble, biodegradable, and biocompatible polypeptide for biological applications; it can facilitate the attachment of cells and proteins by altering the charge of the substrate from negative

* Corresponding authors at: Department of Materials Engineering, Ming Chi University of Technology, New Taipei City, Taiwan; Department of Materials Science and Engineering, National Taiwan University, Taipei, Taiwan.
E-mail addresses: huangyc@mail.mcut.edu.tw (Y. Huang), suwf@ntu.edu.tw (W. Su).

https://doi.org/10.1016/j.reactfunctpolym.2022.105265
Received 30 January 2022; Received in revised form 6 April 2022; Accepted 9 April 2022
Available online 15 April 2022

to positive, and has been used as a nonviral gene delivery vector [16]. PLL not only promotes cell adhesion but also the adsorption of serum and extracellular matrix onto substrates. PLL coating of a substrate can effectively enhance its cell attachment relative to that of the untreated substrate [17–19]. PLL is also often used as a charge enhancer or coating agent, enhancing not only cell adhesion but also cell growth, differentiation, and life span.

Three-dimensional aligned PBG scaffolds can effectively enhance the viability of PC-12 cells and the extension of neurites, due to the presence of their glutamate-like neurotransmitter moieties, which promote synaptic transmission and neurogenesis. After partially hydrolyzing the benzyl glutamate units of a PBG polymer, the exposed carboxylic acid groups can increase the hydrophilicity and cell viability [20]. PC-12 cells adhere poorly to polystyrene (PS) cell culture plates, but they readily attach to hydrophilic substrates [21,22]. They are anchoring-dependent cells; their degree of neurite outgrowth depends on how well they attach to the substrate [23]. Thus, for cell culturing, a PLL coating is typically applied to a plate to increase the adhesion and attachment of PC-12 cells, followed by placing a growth factor (material) on top of the PLL coating or in the cell culture solution; this two-step procedure not only is time-consuming and wasteful but also increases the likelihood of experimental errors.

Ideally, a single polypeptide coating could be used to simultaneously improve the cell adhesion and viability of PC-12 neuron cells (or other cells) on a tissue engineering scaffolds. *Co*-polypeptides generally combine the characteristics of their homo-polypeptides. For example, glatiramer acetate (GA) is a random copolymer of glutamic acid, lysine, alanine, and tyrosine that has been used for the treatment of patients with multiple sclerosis (MS) [24]. Random *co*-poly(amino acids) composed of glutamic acid, lysine, and alanine have been used as additives for the biomimetic mineralization of $CaCO_3$ [25]. The literature has reported that cells have a stronger interaction between cells and L-type polypeptides as compared with D-type polypeptides through stereospecific recognition between cells and polypeptides [26–28]. We would like to have the biopolymers are biocompatible and biodegradable with good cell activity and adhesion, thus we choose L-type amino acids to synthesize copolymers for this research. And all L-type repeating unit can also make the packing of the polymer chain more regularly relative to the combination of L and D-type, and embedding D-type repeating unit.

To achieve a single applicable coating system, in this study we synthesized peptide copolymers containing units of the neurotransmitter glutamate and units of the cell adhesion promoter lysine. To determine the best copolymer, we investigated the effects of the chemical structure and composition on cell adhesion and growth. Furthermore, we partially hydrolyzed the best copolymer to induce net charge and, thereby, increase its cell adhesion and recognition.

2. Experimental section

2.1. Chemicals

The following chemicals and materials were used as received: L-glutamic acid γ-benzyl ester (Sigma–Aldrich), N_ε-carbobenzoxy-L-lysine (Sigma–Aldrich), N_ε-butyloxycarbonyl-L-lysine (Sigma–Aldrich), triphosgene (Sigma–Aldrich), sodium (Sigma–Aldrich), ethyl acetate (EA; Acros), dichloroacetic acid (DCA; Acros), 33 wt% HBr in acetic acid (Acros), tetrahydrofuran (THF; Sigma–Aldrich), benzene (Sigma–Aldrich), methanol (Sigma–Aldrich), dimethylacetamide (DMAC; Sigma–Aldrich), d-chloroform (Merck), d-trifluoroacetic acid (Acros), ether (Macron), hexane (Uni-onward Corp. Taiwan), Dulbecco's modified Eagle's medium high glucose (DMEM-HG; 12,100–046; Gibco), Roswell Park Memorial Institute 1640 medium (RPMI-1640; SH30011.02; Hyclone), DMEM/F12 medium (Gibco), phosphate-buffered saline (PBS; P4417; Sigma–Aldrich), Alamar Blue cell cytotoxicity assay (BUF102A, AbD Serotec), fetal bovine serum (FBS; 04–001-1A; Gibco), horse serum (HS; 16,050,122; Gibco), antibiotic antimycotic solution—penicillin/streptomycin/amphotericin B (PSA, A5955; Sigma–Aldrich), 0.25% trypsin protease (03–051-5B, HyClone), dimethyl sulfoxide (DMSO; SU01551000; Sigma–Aldrich), bovine serum albumin (BSA; A9418; Sigma), live/dead viability/cytotoxicity kit (L3224, Molecular Probes).

2.2. Characterization

NMR spectroscopy (Bruker; DPX400) was used to determine the chemical structures of the monomers and copolymers. FTIR spectroscopy (PerkinElmer; Spectrum 100) was used to determine the compositions of the copolymers. Gel permeation chromatography (GPC; Waters; Breeze 2) was used to determine the molecular weights of the copolymers. The mobile phase solvent of the GPC used in this research was DMF, and polystyrene was used as the standard for the calibration curve. From the GPC trace, it can be seen that the peak at 11–13 min represents the DMF solvent, and we integrate the major peak to determine the molecular weight. A spin coater (SP-480CA; Yongyi) was used to fabricate the polymer films. Water contact angle analysis (Model 100SB, Sindatek) was performed to measure the hydrophilicity of the polymer film surfaces. Bio-atomic force microscopy (Bio-AFM, Bruker, tapping mode) was used to measure the roughness of the polymer film surfaces. The zeta potential of hydrolyzed copolymer was measured by dynamic light scattering (DLS; Brookhaven 90Plus nanoparticle size analyzer). The hydrolyzed copolymer solid was uniformly dispersed in water at a concentration of 0.01%, and used to measure the zeta potential.

Instruments for studying the cell viability and cytotoxicity included a centrifuge (Kubota; 2420), incubator (ESCO; 81,022), thermostatic water bath (DSB500E, Digisystem), laminar flow hood (ESCO; class II type A2), 4 °C refrigerator (SC122, Azotech), −20 °C refrigerator (SCF-141 K, Sanyo), optical microscope (DMI3000 B; Leica), confocal microscope (TCS SP5 II, Leica), and absorbance microplate reader (ELx800, BioTek).

Molecular simulation software, Cambridge Serial Total Energy Package (CASTEP) of Materials Studio 4.3, was used to investigate the structure conformation of protecting group of lysine which is basis on the density functional theory. The angle between protecting group and lysine of structure conformation was determined by geometry optimization.

2.3. Nomenclature

The following nomenclature is used throughout this study: *N*-carboxyanhydride, NCA; poly(γ-benzyl-L-glutamate), PBG; poly(N_ε-carbobenzoxy-L-lysine), PCBZL; poly(N_ε- *tert*-butoxycarbonyl -L-lysine), PBOCL; γ-benzyl glutamate-*N*-carboxyanhydride, BG-NCA; N_ε-carbobenzoxy-L-lysine-*N*-carboxyanhydride, CBZL-NCA; N_ε-*tert*-butoxycarbonyl-L-lysine-*N*-carboxyanhydride, BOCL-NCA; poly((N_ε-carbobenzoxy-L-lysine)$_m$–*co*–(γ-benzyl-L-glutamate)$_n$), P((CBZL)$_m$-co-(BG)$_n$) (*m*:*n* = 1:9, 1CBZL9BG; *m*:*n* = 3:7, 3CBZL7BG; *m*:*n* = 5:5, 5CBZL5BG; *m*:*n* = 7:3, 7CBZL3BG; *m*:*n* = 9:1, 9CBZL1BG); poly((N_ε-t-butoxycarbonyl-L-lysine)$_m$–*co*–(γ-benzyl-L-glutamate)$_n$), P((BOCL)$_m$-co-(BG)$_n$) (*m*:*n* = 1:9, 1BOCL9BG; *m*:*n* = 3:7, 3BOCL7BG; *m*:*n* = 5:5, 5BOCL5BG; *m*:*n* = 7:3, 7BOCL3BG; *m*:*n* = 9:1, 9BOCL1BG); poly((N_ε-carbobenzyloxy-L-lysine)$_{43}$–*co*–(L-lysine)$_{57}$)$_{50}$–*co*–((γ-benzyl-L-glutamate)$_{56}$–*co*–(L-glutamic acid)$_{44}$)$_{50}$), 5BL57-5BGA44.

2.4. P((CBZL)$_m$-co-(BG)$_n$) copolymers

The synthesis and characterization of the monomers BG-NCA [15], CBZL-NCA [29], and BOCL-NCA [30] are provided in the Supporting Information. The procedure for polymerization is described below.

Dried NCA monomers and anhydrous benzene (ratio: 1 g of monomer to 100 mL of benzene) were added to a dry 500-mL flask under N_2 at room temperature. Sodium methoxide was prepared from sodium

(50–70 mg) in methanol (5 mL) and benzene (15 mL) in a 100-mL round-bottom flask under N_2 at room temperature. The solution of sodium methoxide was then added to the solution of the monomers to initiate the polymerization at room temperature for 3 days. The molar ratio of monomer to initiator was 100:1. The resulting mixture was poured into ether (1000 mL) to give a precipitate, which was dried under vacuum at 40 °C to obtain the final copolymer [15]. Five copolymers of P((CBZL)$_m$-co-(BG)$_n$) were prepared with feeding ratios of CBZL to BG of 1:9, 3:7, 5:5, 7:3, and 9:1. Each copolymer was obtained in a yield of approximately 90%. The chemical structures of P((CBZL)$_m$-co-(BG)$_n$) were confirmed using NMR and FTIR spectroscopy (Figs. S4 and S6). The characteristic NMR spectral chemical shifts (δ) of P((CBZL)$_m$-co-(BG)$_n$) (Fig. S4) were 7.50 (a; ArH), 5.37 (b; CH_2-benzylic), 4.96 (c; C—H, amide of glutamate), 4,76 (c′; C—H, amide of lysine), 3.37 (d; γ-CH_2 of glutamate), 2.73 (e; ε-CH_2 of lysine), 2.22 (f: β-CH_2), and 1.47 (g; γ, δ-CH_2) ppm. FT-IR (ATR, cm^{-1}): 3287 (NH), 2920 (C—H), 1734 (ester, C═O), 1650 (amide, NHC═O), 1543 (amide, NHC═O), 1245 (CBZ, C—O), 1165 (Bn, C—O), 745, 698 (phenyl) (Fig. S6).

2.5. P((BOCL)$_m$-co-(BG)$_n$) copolymers

Dried NCA monomers and anhydrous benzene (ratio: 1 g of monomer to 100 mL of benzene) were added to a dry 500-mL flask under N_2 at room temperature. Sodium methoxide was prepared from sodium (50–70 mg) in methanol (5 mL) and benzene (15 mL) in a 100-mL round-bottom flask under N_2 at room temperature. The solution of sodium methoxide was then added to the solution of the monomers to initiate the polymerization at room temperature for 3 days. The molar ratio of monomer to initiator was 1:100. The resulting mixture was poured into ether (1000 mL) to give a precipitate, which was dried under vacuum at 40 °C to obtain the final copolymer [15]. Five copolymers of P((BOCL)$_m$-co-(BG)$_n$) were prepared with feeding ratios of BOCL to BG of 1:9, 3:7, 5:5, 7:3, and 9:1. Each copolymer was obtained in a yield of approximately 86%. The chemical structures of P((BOCL)$_m$-co-(BG)$_n$) were confirmed using NMR and FTIR spectroscopy (Figs. S5 and S7). The characteristic NMR spectral chemical shifts (δ) of P((BOCL)$_m$-co-(BG)$_n$) (Fig. S5) were 7.50 (a; ArH), 5.37 (b; CH_2-benzylic), 4.96 (c; C—H, amide of glutamate), 4.76 (c′; C—H, amide of lysine), 3.37 (d; γ-CH_2 of glutamate), 2.73 (e; ε-CH_2 of lysine), 2.22 (f; β-CH_2), 1.47 (g; γ, δ-CH_2), and 1.65 (i; CH_3 of BOC group) ppm. FTIR (ATR, cm^{-1}): 3287 (N—H), 2920 (C—H), 1734 (ester, C═O), 1650 (amide, NHC═O), 1543 (amide, NHC═O), 1392, 1366 (BOC, CH_3), 1165 (Bn, C—O), 745, 698 (phenyl) (Fig. S7).

2.6. Hydrolyzed copolymers

The solid copolymer (500 mg) was dissolved in dichloroacetic acid (12.5 mL) with stirring at room temperature for 24 h. 33 wt% Hydrogen bromide in acetic acid (370 μL) was added and then the mixture was stirred at 31 °C for 30 min. The product was precipitated out in ether (400 mL) and washed for 30 min. The precipitate was collected by filtration and purified by repeated dissolving in methanol (50 mL) and precipitating in ether at least five times. The purified solid was collected by filtration and vacuum-dried at 40 °C overnight to give the final product (yield: 70.4%). The extent of hydrolysis was analyzed using FTIR spectroscopy (not NMR spectroscopy, because there were no good solvents). The FTIR spectral analysis involved measuring the change in the height of the signals for the ester functional groups [C(=O)C–O] to

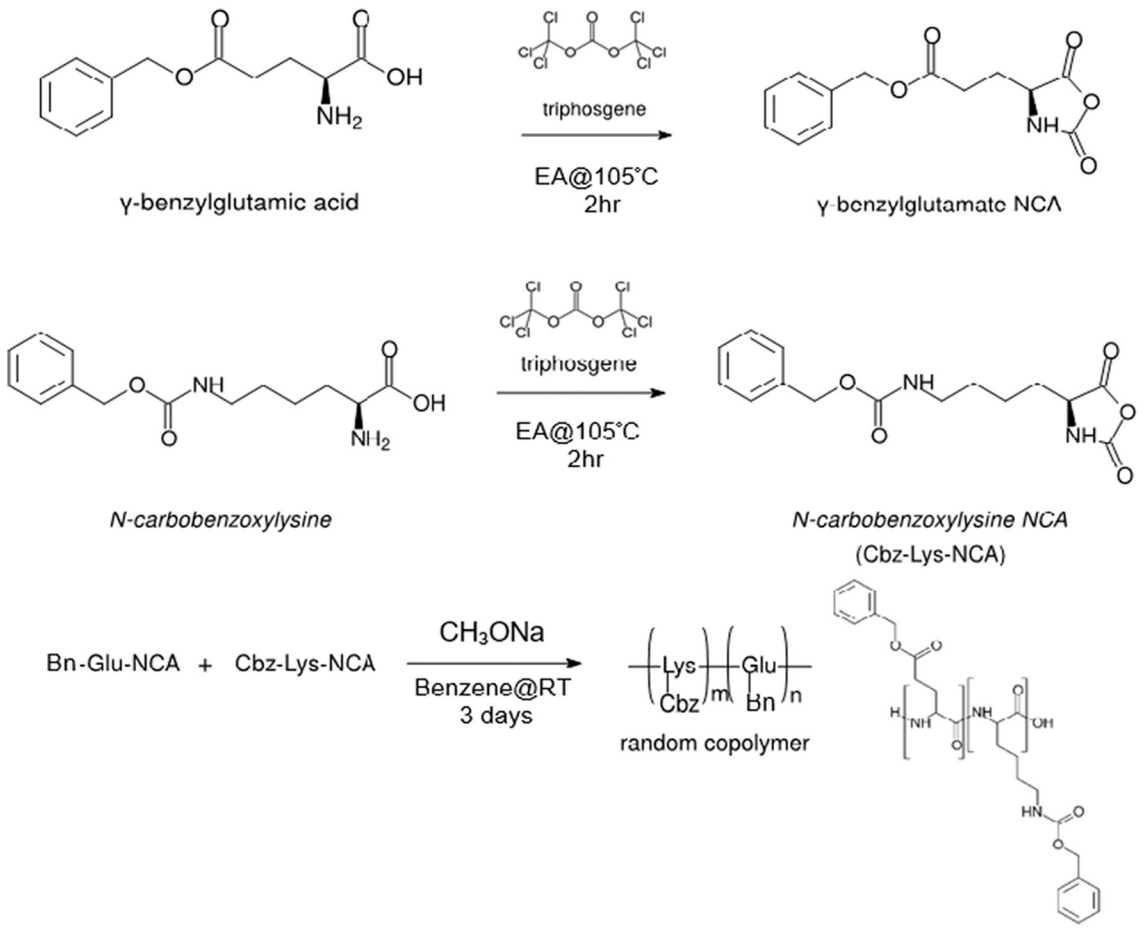

Fig. 1. Chemical reactions used for P((CBZL)$_m$-co-(BG)$_n$) copolymer synthesis.

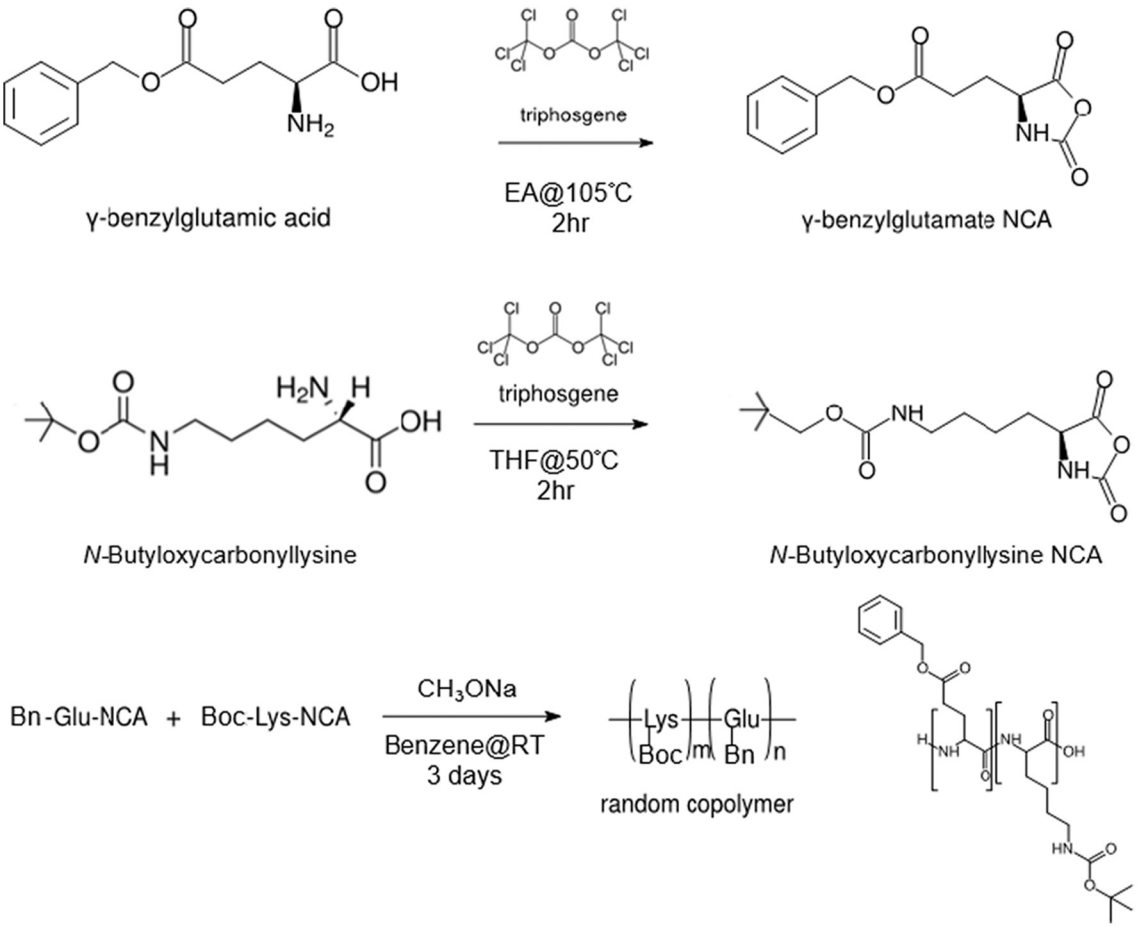

Fig. 2. Chemical reactions used for P((BOCL)$_m$-co-(BG)$_n$) copolymer synthesis.

calculate the hydrolysis rate. Decreases in the intensities of the signals at 1243 and 1165 cm^{-1} represented deprotection of the CBZ and Bn units. All of the peaks were normalized with respect to the peak at 1545 cm^{-1}, which represented the amide groups on the main chain (Fig. S8).

2.7. Polymer films

Homogenous solutions (20 wt%) of PBG, PCBZL, PBOCL, P((CBZL)$_m$-co-(BG)$_n$), and P((BOCL)$_m$-*co*-(BG)$_n$) were prepared by dissolving the solid polymers overnight in a mixture (1:2, *v*/v) of *N*,*N*-dimethylacetamide (DMAc) and acetone. The polymer films were fabricated by spin-coating the respective solution onto cover slip substrates, first at 2000 rpm for 40 s and then at 3000 rpm for 50 s. The films were vacuum-dried at 40 °C overnight.

2.8. Cytotoxicity tests

The cytotoxicities of the polymer films were examined using a live/dead assay. PC-12 and ARPE-19 cells were seeded onto the polymer films in 24-well PS cell culture dishes. (PC-12 cell density: 20,000 cells/cm^2; ARPE-19 cell density: 5000 cells/cm^2). PC-12 cells were cultured in RPMI-1640 medium and ARPE-19 cells were cultured in DMEM/F12 medium with 10% (*v*/v) HS, 5% (v/v) FBS, and 1% (v/v) PSA at 37 °C under 5% CO_2. After 5 days, the culture medium was removed, and the film sample was washed with PBS. The cultured cells were then stained with 0.05% (v/v, in PBS) calcein-AM for live cells and 0.2% (v/v, in PBS) ethidium homodimer-1 (EthD-1) for dead cells, at room temperature for 45 min. After another PBS washing, the cells were again immersed in fresh PBS for examination using fluorescence optical microscopy.

2.9. Cell viability tests

The cell viabilities of the copolymer films were examined using an Alamar Blue assay. PC-12 and ARPE-19 cells were seeded onto the polymer films in 24-well PS cell culture dishes (PC-12 cell density: 20,000 cells/cm^2; ARPE-19 cell density: 5000 cells/cm^2). The PC-12 cells were cultured in RPMI-1640 medium and the ARPE-19 cells were cultured in DMEM/F12 medium with 10% (*v*/v) HS, 5% (v/v) FBS, and 1% (v/v) PSA at 37 °C under 5% CO_2 for 1, 3, or 5 days. After 1 day, the culture medium was removed and the samples were washed with PBS. Diluted Alamar Blue solution (10% v/v, in DMEM) was then added to the wells containing cells; one well, without cells, served as a blank. The cells were then incubated at 37 °C under 5% CO_2 for reaction with the Alamar Blue reagent. After 4 h, the solution was pipetted out to another 96-well plate to test the absorption at 570 and 600 nm. The samples were then washed with PBS and added with culture medium to continue the cell culturing into the third and fifth days. The dye reduction percentage was calculated using Eq. (S1) and normalized to the value obtained on day 1 by setting the day 1 value to be a cell viability index of 1.0.

3. Results and discussion

3.1. Synthesis and characterization of polypeptide copolymer

The synthesis of the copolymers began with the preparation of the NCA monomers of glutamic acid and lysine, respectively. The COOH group of the side chain of glutamic acid and the NH_2 group of the side chain of lysine were protected separately prior to NCA synthesis. To

Table 1
GPC data of the synthesized homopolymers and P((CBZL)$_m$-co-(BG)$_n$) and P((BOCL)$_m$-co-(BG)$_n$) copolymers.

Polymer	Mw (kDa)	Mn (kDa)	PDI (Mw/Mn)
PBG	256	212	1.21
PCBZL	293	248	1.18
PBOCL	278	222	1.25
1CBZL9BG	290	193	1.50
3CBZL7BG	260	217	1.20
5CBZL5BG	289	228	1.27
7CBZL3BG	243	231	1.05
9CBZL1BG	240	231	1.04
1BOCL9BG	260	255	1.02
3BOCL7BG	250	248	1.01
5BOCL5BG	228	213	1.07
7BOCL3BG	225	186	1.21
9BOCL1BG	237	214	1.11

study the effects of the chemical structures and compositions of the copolymers on their interfacial characteristics during cell culturing, we choose the benzyl (B) protecting group for glutamic acid and two protecting groups—N$_\varepsilon$-t-butyloxycarbonyl lysine (BOCL) and N$_\varepsilon$-carbobenzoxy lysine (CBZL)—for lysine. We then performed ring-opening copolymerizations with various compositions of the NCA derivatives of glutamate and lysine, using sodium methoxide as a strong base initiator at a monomer-to-initiator ratio of 100:1. Polymers of high molecular weight (on the order of hundreds of thousands) and narrow polydispersity were produced, suitable for processing into films and fibers. Figs. 1 and 2 display the chemical reactions used for the copolymer synthesis.

The molecular weights of the various polymers were analyzed through gel permeation chromatography (GPC) using dimethylformamide (DMF) as the mobile phase. Table 1 summarizes the results. All the GPC traces of copolymers are very similar. The representative one, the GPC result of copolymer 5CBZL5BG has been added in the Supporting Information as Fig. S9. The small peak before the large peak is the aggregation of polymer molecules caused by polar interaction and hydrogen bonding between single polymer chain [31]. We used nuclear magnetic resonance (NMR) spectroscopy and Fourier transform infrared (FTIR) spectroscopy to evaluate the chemical structures of P((CBZL)$_m$-co-(BG)$_n$) and P((BOCL)$_m$-co-(BG)$_n$). The copolymer compositions were determined using NMR spectroscopy from the relative intensities of the signals for the amide protons of the lysine and glutamate moiety (Table S1); from the FTIR spectra, we established a calibration curve based on the absorption peaks of the individual homopolymers and the homopolymer blends at different compositions (Figs. S10–S12). Fig. 3 presents the results of the NMR spectral analysis. The compositions of the synthesized copolymers (red dots) agreed with the feed compositions of the monomers (blue dots), regardless of the type of monomer. The red and blue dots aligned, indicating that the polymerizations were ideal random copolymerizations without any composition drift. For FTIR spectral characterization, the chemical compositions of the synthesized copolymers were determined from the characteristic peaks of the homopolymers PBG, PCBZL, and PBOCL and from the calibration curve established from polymer blends of various compositions. The intensity ratios of the signals at 1243 cm^{-1} (ester of CBZ) and 1165 cm^{-1} (ester of B) of the synthesized P((CBZL)$_m$-co-(BG)$_n$) were compared with those in the calibration curve in Fig. S11. The intensity ratios of the signals at 1366 cm^{-1} (CH$_3$ of BOC) and 696 cm^{-1} (phenyl group of B) of the synthesized P((BOCL)$_m$-co-(BG)$_n$) were compared with those in the calibration curve in Fig. S12. The actual intensity ratios of the synthesized copolymers were also in the line with those of the homopolymer blends (Figs. S13 and S14). The NMR and FTIR spectral data confirmed that the compositions of the copolymers were closely related to the feed ratios of their monomers; thus, the copolymerizations were ideal copolymerizations.

3.2. Surface characteristics of copolymer films

We used water contact angle measurements and atomic force microscopy to evaluate the surface characteristics of the copolymer films. Table 2 summarizes the results. As expected, the contact angle of PBG decreased upon incorporation of the hydrophilic lysine moiety. At 10 mol% of lysine, the samples 1CBZL9BG and 1BOCL9BG had contact angles of 77.8 ± 1.8° and 76.0 ± 0.8°, respectively, relative to a value of 86.6 ± 2.8° for PBG. Interestingly, for larger amounts of lysine in the copolymer, the type of protecting group on the lysine moiety affected the hydrophilicity. The trend was reversed when the amount of BOCL was equal to or greater than 50 mol%, with the contact angles increasing to 81.8 ± 0.5° for 5BOCL5BG and 99.5 ± 0.8° for 9BOCL1BG. We speculate that during the spin-coating process, the bulky *tert*-butoxy groups, having a large bond angle of 113.95°, in the polymer chains [Fig. 4(b)] would tend to place themselves toward the air, thereby causing the polymer chains to pack unevenly and result in a hydrophobic coating on a hydrophilic glass substrate. In contrast, the carbobenzoxy unit, containing a C═O group and a benzene ring, would tend to lay flat with a smaller bond angle of 80.71° [Fig. 4(a)], resulting in evenly packed polymer chains and no effect on the hydrophilicity of P

Table 2
Surface characteristics of films of homopolymers and copolymers.

Polymer	Contact angle (°)	Surface roughness (nm)
PBG	86.6 ± 2.8	37.4 ± 8.3
1CBZL9BG	77.8 ± 1.8	32.8 ± 5.6
5CBZL5BG	69.8 ± 4.4	37.2 ± 8.3
9CBZL1BG	69.2 ± 2.3	37.2 ± 14.2
PCBZL	73.6 ± 0.5	35.4 ± 5.9
1BOCL9BG	76.0 ± 0.8	68.1 ± 13.4
5BOCL5BG	81.8 ± 0.5	89.3 ± 17.5
9BOCL1BG	99.5 ± 0.8	95.9 ± 22.0
PBOCL	96.2 ± 0.9	197 ± 46.7

Three samples were examined for each material.

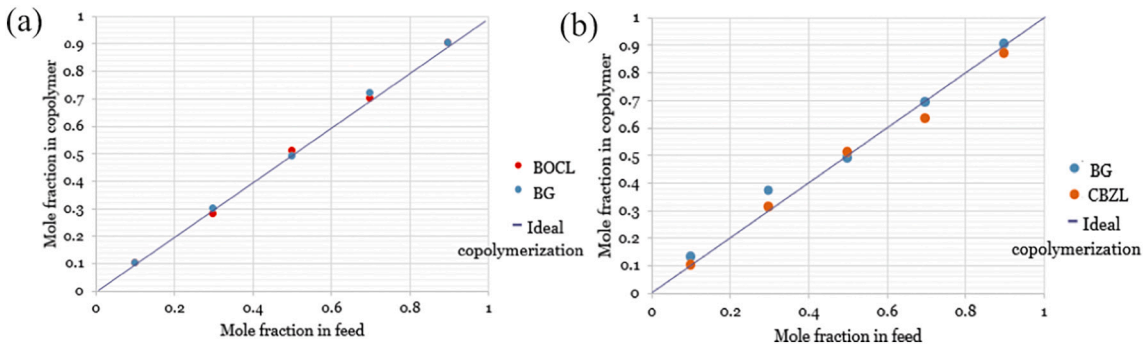

Fig. 3. Plots of copolymer composition with respect to feed composition for the copolymers (a) P((CBZL)$_m$-co-(BG)$_n$) and (b) P((BOCL)$_m$-co-(BG)$_n$).

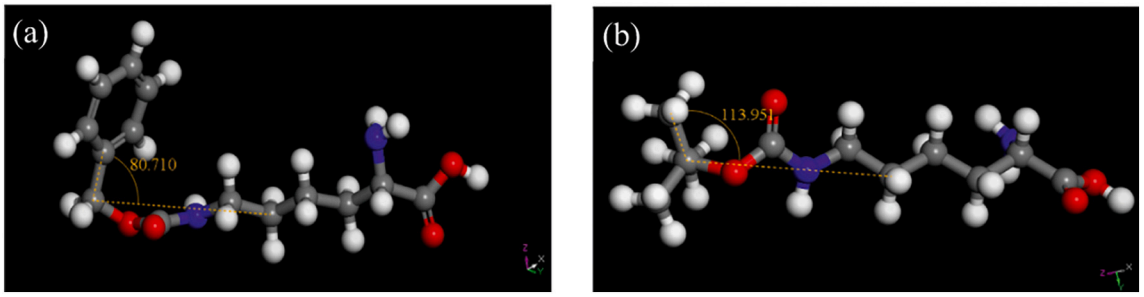

Fig. 4. Models of the molecular structures featuring (a) CBZ and (b) BOC protecting groups for the lysine moiety.

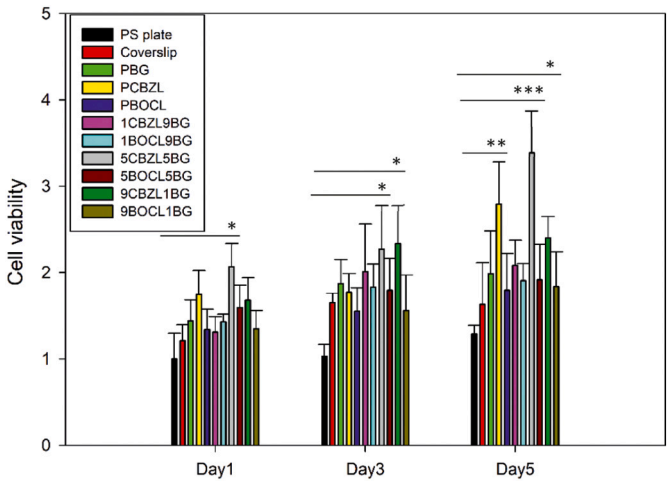

Fig. 5. Cell viability of PC-12 cells after 5-day cultures. Experiments with each group were repeated three times. The cell viability index was obtained by normalizing all of the values with respect to the values on day one in PS culture dishes. Kruskal-Wallis H test: *** indicates $P < 0.001$, ** indicates $P < 0.01$ and * indicates $P < 0.05$.

((CBZL)$_m$-*co*-(BG)$_n$) on glass [32]. The surface roughness of the copolymers followed the same trends. All of the copolymers containing BOCL units had rough surfaces, even at a low molar ratio of 10% (cf. 68.1 ± 13.4 nm for 1BOCL9BG with 37.4 ± 8.3 nm for PBG). The neat PBOCL had an extremely high surface roughness of 197 ± 46.7 nm, as expected. The AFM images of homopolymers and copolymers are shown in Fig. S15. The images of BOCL-containing copolymers exhibit porous structure which results in more hydrophobic surface as compared to CBZL-containing group copolymers. Under the same film preparation conditions, the porous structure may be resulted from the BOCL copolymers chain containing large bond angle (114°) and bulky group of tert-butoxy in lysine repeating unit. Thus, the BOCL copolymers pack polymer chains loosely as compared with the CBZL copolymers containing small bond angle (81°) and flat group of benzyl in lysine repeating unit. Therefore, the polymer chains of CBZL copolymers are more uniformly packed, close to flat, and have little effect on the surface roughness of the films.

3.3. Cell viability and cytotoxicity of polymer films

We used an Alamar Blue assay to evaluate the cell viability of the polymer films. Initially, we employed PC-12 cells. The cell viability index was obtained by normalizing all data with respect to the day-one values in a PS cell culture dish. Fig. 5 presents the cell viability indexes on days 1, 3, and 5 for various polymer films. The cell viabilities of all samples increased upon increasing the number of days, implying good biocompatibility for the films. The cell viabilities of all of the materials were higher than that of the control group PS plate. Thus, the PC-12 cells could adhere well to the cover slip without any surface treatment. Among the homopolymers, PCBZL had cell viability higher than those of PBG and PBOCL, consistent with its greater hydrophilicity (lowest contact angle) and lowest surface roughness. At 10 mol% incorporation of the two lysine derivatives into PBG, the copolymers P((CBZL)$_m$-co-(BG)$_n$) and P((BOCL)$_m$-co-(BG)$_n$) exhibited almost the same cell viability as PBG. When the amount of CBZL was 50 mol% or greater, the cell viability was higher than that of PBG. In contrast, when the amount of BOCL was 50 mol%, the cell viability decreased, because its rougher surface resulted in poor cell adhesion, which affected cell growth. 5CBZL5BG provided the greatest cell viability among all of our

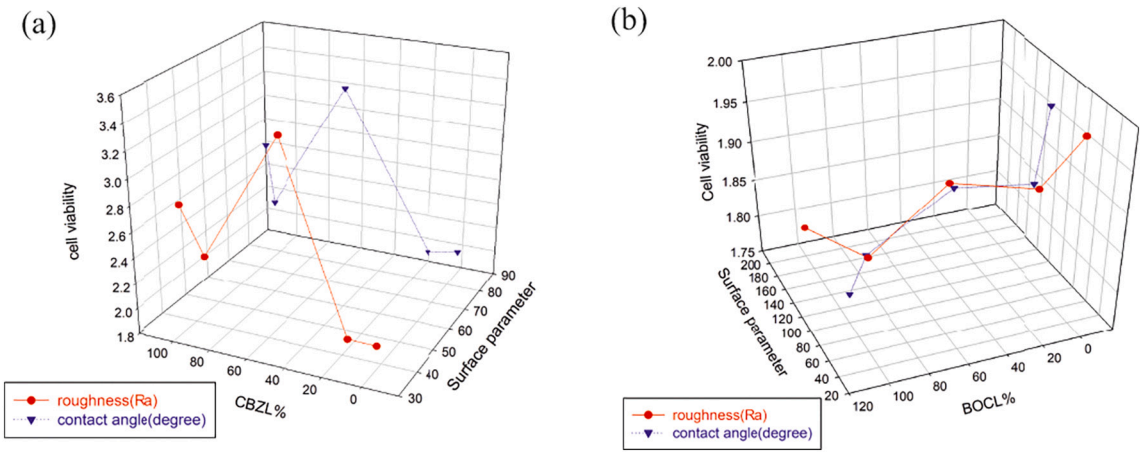

Fig. 6. 3D plots of the effects of copolymers chemical compositions on the cell viability, roughness, and contact angle after 5-day cultures on (a) P((CBZL)$_m$-co-(BG)$_n$)) and (b) P((BOCL)$_m$-co-(BG)$_n$)) films.

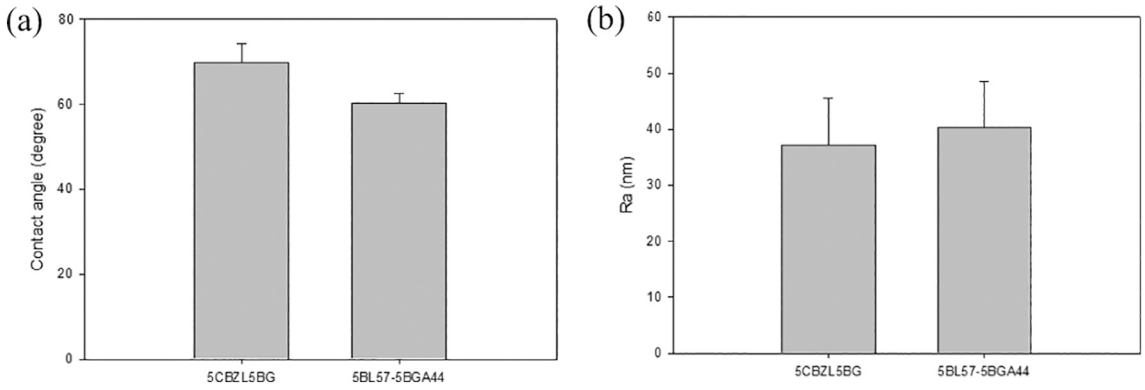

Fig. 7. (a) Surface roughness and (b) contact angles of the polymer films 5CBZL5BG and 5BL57-5BGA44. Three samples were examined for each material.

examined copolymer films. Interestingly, the cell viability of 5CBZL5BG was also greater than that of PCBZL. Fig. S16 displays the cell viability on day 5 for the various polymer films, with statistical significance. The results suggest that good cell viability required both good cell adhesion and good cell growth. The glutamate moiety of 5CBZL5BG acted as a neurotransmitter to increase nerve cell stimulation and growth.

To examine the correlations of the cell viabilities with respect to the copolymer structures, compositions, and surface characteristics, we constructed 3D plots (Fig. 6). The chemical structures and compositions of the copolymers influenced the surface characteristics, which affected the cell viability. A balance among the chemical structure and composition, hydrophilicity, and surface roughness was required to ensure high cell viability.

Fig. 6(a) reveals that the amount of CBZL in the copolymer affected the surface characteristics and cell viability. For this series of polymers—PBG, PCBZL, and P($(CBZL)_m$-co-$(BG)_n$)—the surfaces were flat, with roughness ranging from 30 to 40 nm. Both BG and CBZL contain relatively flat benzyl protecting groups, which had little effect on the surface roughness of their polymer films. Nevertheless, the presence of amide groups in the CBZL units of the polymer could potentially increase the hydrophilicity and cell viability. At a 50% molar concentration of CBZL in the copolymer, 5CBZL5BG exhibited the highest cell viability among all of our tested copolymers. We speculated that cell stimulation induced by the glutamate moieties of 5CBZL5BG took effect to promote cell growth on the adhered cells. Thus, the cells had to adhere well to the substrate first before any growth factor could then exhibits its effective function. The cell viability of 9CBZL1BG was lower than that of 5CBZL5BG after 5 days of culture (Fig. S17). Although 9CBZL1BG possessed good hydrophilicity and a flat surface, it featured only 10% glutamate to promote PC-12 growth. Fig. 6(b) presents the correlations of the cell viability with respect to the surface characteristics and copolymer compositions for the series of polymers PBG, PBOCL, and P($(BOCL)_m$-*co*-$(BG)_n$). Interestingly, the bulky *tert*-butyl protecting group (tetrahedral bond at 113.95°) of the lysine residue had opposite effects on the hydrophilicity and surface roughness when compared with those of the relatively flat carbobenzoxy protecting group (C═O and benzyl bonds at 80.71°). The bulky group decreased the hydrophilicity and increased the surface roughness and, thus, the cell viability decreased upon incorporating the BOCL moiety into PBG (Fig. S18). This finding confirmed that cell adhesion was the primary factor behind cell viability on the cell culture plate. Fig. 6(a) and (b) also indicate that the chemical structure of the copolymer affected the cell viability, in addition to the effect of the composition of the copolymer.

We used a live/dead assay to determine the cytotoxicity of the polymer films toward PC-12 cells. Fig. S19 presents the live/dead situation of cells on the polymer films after a 5-day culture. Red dead cells were hardly observable after the 5-day culture, indicating that the homopolymer and copolymer films had low cytotoxicity. More live cells appeared on the PCBZL film [Fig. S19(c)] than on the PBG film [Fig. S19 (a)] and much more than on the PBOCL film [Fig. S19(e)]. These findings are consistent with the cell viabilities determined from the point of view of cell adhesion. The 5CBZLBG film, which had the optimal chemical structure and copolymer composition, possessed the highest affinity toward cells and displayed the highest cell population. The poor adhesion of copolymers containing BOCL [Fig. S19(g), S19(i), and S19 (q)] also resulted in live cell populations lower than those of copolymers containing CBZL. Thus, the cells survived much better on the polypeptides that provided good cell adhesion. The polymers having flat and hydrophilic surfaces, such as the CBZL series of copolymers, performed this function well [Fig. S19(c), S19(k), and S19(o)]. In this study, we did not perform any additional common cell adhesive coating procedure (e.g., using either PLL or matrigel). Thus, a single copolymer, designed with a specific chemically active moiety, acting as a coating for a culture plate could indeed achieve both high adhesion and cell survivability, potentially improving the cell culture efficiency and minimizing experimental errors.

3.4. PC-12 and ARPE-19 cell viabilities and cytotoxicities on 5CBZL5BG and partially hydrolyzed 5CBZL5BG copolymer films

Partial hydrolysis of polypeptides containing protecting groups can increase the adhesion and affinity of PC-12 cells, due to the presence of net charge on the polypeptide chains [14,19]. We explored this phenomenon using our optimal copolymer, 5CBZL5BG. Because the rate of hydrolysis of CBZ is faster than that of B [33], we could partially hydrolyze 5CBZL5BG to obtain a polymer presenting net positive charge. Accordingly, we used 25.35 wt% HBr to hydrolyze the copolymer for 30 min. The extent of hydrolysis was monitored using FTIR spectroscopy, because it is widely known method [34,35]. The decrease of peak intensity of ester linkage side chain of repeating unit can be cleared observed by FT-IR after the sample being hydrolyzed as shown in Fig. S8. The result shows that 57% of the CBZL units and 44% of the BG of 5CBZL5BG were hydrolyzed. The zeta potential of hydrolyzed 5CBZL5BG was measured by DLS as shown in Fig. S20. The average value of measured zeta potential is as high as +41.69 mV, which means that the copolymer has good stability and dispersion in aqueous solution with positive charge. This result is consistent with the result of FT-IR which indicates the copolymer contains more lysine unit than glutamic acid unit. The hydrolyzed copolymer had the formula $((PCBZL)_{43}(PLL)_{57})_{50}$-co-$((PBG)_{56}(PGA)_{44})_{50}$, denoted here as 5BL57-5BGA44. This polymer acted as a charge enhancer and increased the adhesion of PC-12 cells on the substrate. As expected, the hydrophilicity and surface roughness of the hydrolyzed copolymer were increased, due to the presence of the net positive charge, without affecting surface roughness (Fig. 7).

We used Alamar Blue and live/dead assays to evaluate the viability and toxicity of copolymer films of 5CBZL5BG and 5BL57-5BGA44 toward PC-12 cells (Figs. 8 and 9). The cell viability index was obtained by

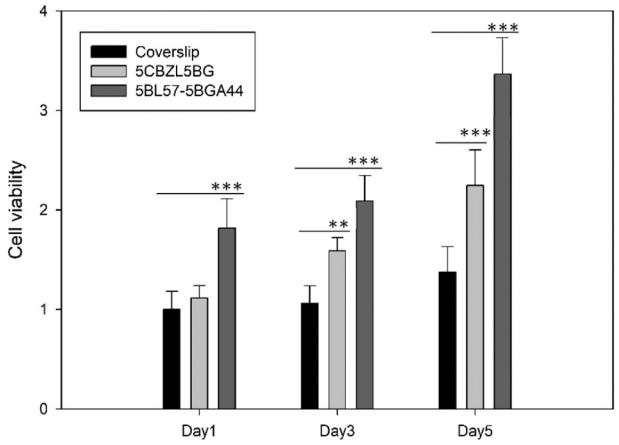

Fig. 8. Cell viability of PC-12 cells on polymer films for 5-day culture. Experiments with each group were repeated three times. Kruskal-Wallis H test: *** indicates $P < 0.001$, ** indicates $P < 0.01$ and * indicates $P < 0.05$.

normalizing all data with respect to the day-one values for the cover slip. Fig. 8 presents the cell viability indexes on days 1, 3, and 5 for the polymer films of 5CBZL5BG and 5BL57-5BGA44 in a PS cell culture dish. The cell viabilities of the two films were higher than that of the cover slip (control) and increased upon increasing the number of days, indicating that both materials had high biocompatibility. Notably, however, the cell viability of 5BL57-5BGA44 was higher than that of the material prior to hydrolysis. The live/dead assay revealed that there were more live cells on 5BL57-5BGA44 than on 5CBZL5BG, with dead cells being almost completely absent (Fig. 9). The results are consistent with the greater contact angle and similar roughness of the hydrolyzed 5BL57-5BGA44, relative to those of 5CBZL5BG. Furthermore, the hydrolyzed copolymer possessed net positive charge, which increased both the hydrophilicity of the surface and the degree of cell recognition.

To confirm the applicability of our copolymers for cell culturing, we further investigated their cell viability and cytotoxicity using APRE-19 cells (adult retinal pigment epithelial cell). The cell viability index was obtained by normalizing all of the data with respect to the day-one

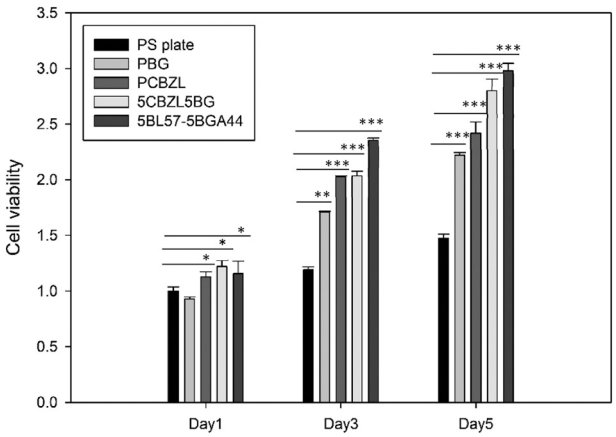

Fig. 10. Cell viability of ARPE-19 cells on polymer films for 5-day culture. Experiments with each group were repeated three times. Kruskal-Wallis H test: *** indicates $P < 0.001$, ** indicates $P < 0.01$ and * indicates $P < 0.05$.

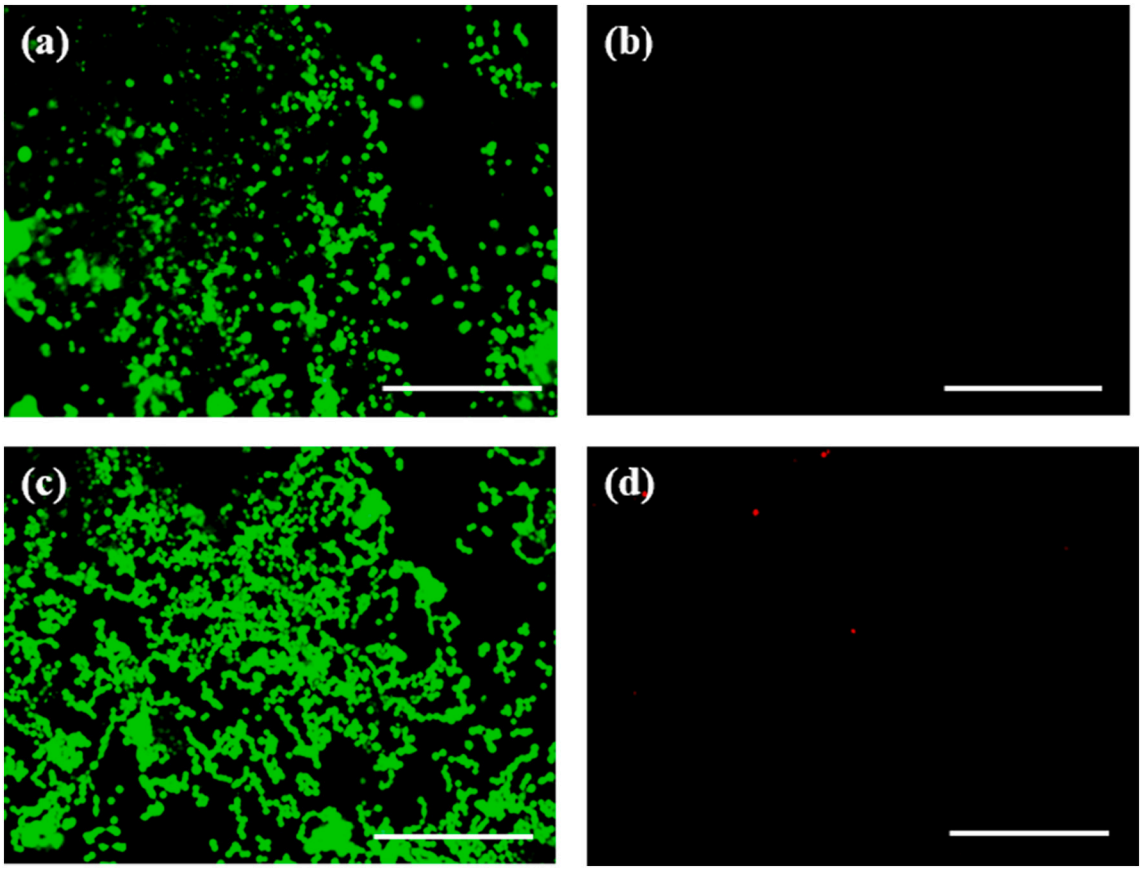

Fig. 9. Representative live/dead fluorescence microscopy images of PC-12 cells after 5-day culture. Green: live cells on films of (a) 5CBZL5BG and (c) 5BL57-5BGA44. Red: dead cells on films of (b) 5CBZL5BG and (d) 5BL57-5BGA44. Scale bars: 500 μm. (For interpretation of the references to colour in this figure legend, the reader is referred to the web version of this article.)

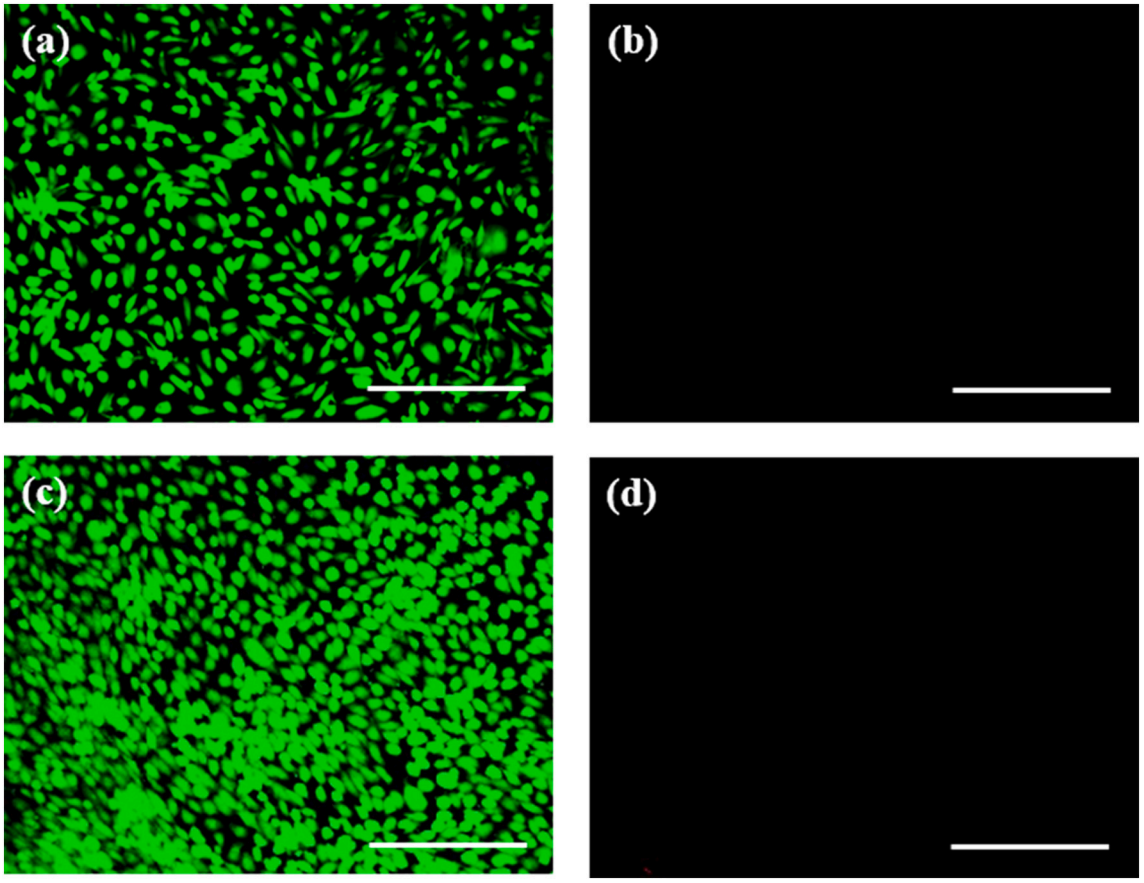

Fig. 11. Representative live/dead fluorescence microscopy images of ARPE-19 cells after 5-day culture. Green: live cells on films of (a) 5CBZL5BG and (c) 5BL57-5BGA44. Red: dead cells on films of (b) 5CBZL5BG and (d) 5BL57-5BGA44. Scale bar: 500 μm. (For interpretation of the references to colour in this figure legend, the reader is referred to the web version of this article.)

values of a PS culture plate. Fig. 10 displays the cell viability indexes on days 1, 3, and 5 for polymer films of PBG, PCBZL, 5CBZL5BG, and 5BL57-5BGA44. The cell viabilities of all of the films were higher than that of the PS culture plate and increased upon increasing the number of days, revealing that these materials exhibited great biocompatibility. The cell viabilities of the copolymer films increased upon increasing the hydrophilicity, with the surface roughness seeming to have little effect. Nevertheless, 5BL57-5BGA44 displayed the highest cell viability among all of our tested films, presumably because of the exposure of its functional groups and its increase in hydrophilicity after hydrolysis of the copolymer. In the cell viability tests with ARPE-19 cells, the cell viability on the 5BL57-5BGA44 film was not significantly higher than that on the other films, the situation we had observed with the PC-12 cells, possibly related to the strong cell adhesion and fast growth of ARPE-19 cells. The 5BL57-5BGA44 film acted as a charge enhancer and increased the adhesion of the ARPE-19 cells to the substrate. The live/dead assay confirmed that all of the films were non-cytotoxic toward ARPE-19 cells, with more live cells stained than dead cells (Fig. 11). The live/dead assay also revealed that more live cells appeared on the 5BL57-5BGA44 film than on any of the other films, with dead cells being almost completely absent (Fig. 11 and Fig. S21). Thus, the 5BL57-5BGA44 film appears to be a highly biocompatible material displaying strong adhesion and viability for both PC-12 and ARPE-19 cells.

4. Conclusion

We have synthesized various compositions of random *co*-polypeptides by ROP through ideal copolymerization. The coating films made from these copolymers exhibited better biocompatibility and lower cytotoxicity than the PS plate control group. Both the hydrophilicity and surface roughness of a coating influenced the adhesion of cells to the substrate. The incorporation of lysine moiety into the glutamate polymer increased the hydrophilicity of the copolymer film. The nature of the protecting group on the side chain type of the lysine moiety also affected the hydrophilicity and surface roughness of the copolymer film. The films fabricated from copolymers presenting bulky *N*-*tert*-butyloxycarbonyl protecting groups on the lysine moiety possessed rougher surfaces than those presenting relatively flat *N*-carbobenzoxy side groups. The presence of BG moieties in the copolymer films stimulated the growth of cells and further increased the cell viability. Thus, the film of the copolymer 5CBCL5BG, containing equal molar ratios of glutamate and lysine residues, exhibited the best performance—in terms of cell survival, adhesion, and proliferation—among all of our investigated coatings. The cell viability on the film of the copolymer 5CBCL5BG improved further after it had been partially hydrolyzed to possess net positive charge. This study confirms the importance of both the chemical structure and composition of a polymeric coating for cell culturing. These characteristics can affect the surface properties of the coating and, thereby, influence the behavior of cell in culture experiments. Cell adhesion on a coating was the primary factor determining the cell viability, which was improved further by incorporating a cell stimulating moiety into the coating. This study provides guidance for the design of appropriate single coating systems for cell culturing, potentially saving time and materials while also minimizing experimental errors. We except that this new class of novel copolymers has potential applications in tissue engineering in regenerative medicine.

Declaration of Competing Interest

The authors declare that they have no known competing financial interests or personal relationships that could have appeared to influence the work reported in this paper.

Acknowledgements

We thank the financial supports of this research from Ministry of Science and Technology of Taiwan (MOST 108-2221-E-002-027-MY3, MOST 110-2221-E-131-010). We also thank the Department of Materials Science and Engineering and Molecular Imaging Center of National Taiwan University for the use of their instruments.

Appendix A. Supplementary data

Supplementary data to this article can be found online at https://doi.org/10.1016/j.reactfunctpolym.2022.105265.

References

[1] Z. Song, Z. Han, S. Lv, C. Chen, L. Chen, L. Yin, J. Cheng, Synthetic polypeptides: from polymer design to supramolecular assembly and biomedical application, Chem. Soc. Rev. 46 (2017) 6570–6599, https://doi.org/10.1039/c7cs00460e.
[2] K. Numata, Poly (amino acid) s/polypeptides as potential functional and structural materials, Polym. J. 47 (2015) 537–545, https://doi.org/10.1038/pj.2015.35.
[3] M. Zelzer, A. Heise, Determination of copolymerisation characteristics in the N-carboxy anhydride polymerisation of two amino acids, Polym. Chem. 4 (2013) 3896, https://doi.org/10.1039/c3py00431g.
[4] M. Rad-Malekshahi, L. Lempsink, M. Amidi, W.E. Hennink, E. Mastrobattista, Bioconjug, biomedical applications of self-assembling peptides, Chem. 27 (2016) 3–18, https://doi.org/10.1021/acs.bioconjchem.5b00487.
[5] T.J. Deming, Synthetic polypeptides for biomedical applications, Prog. Polym. Sci. 32 (2007) 858–875, https://doi.org/10.1016/j.progpolymsci.2007.05.010.
[6] P. Salas-Ambrosio, A. Tronnet, P. Verhaeghe, C. Bonduelle, Synthetic polypeptide polymers as simplified analogues of antimicrobial peptides, Biomacromolecules. 22 (2021) 57–75, https://doi.org/10.1021/acs.biomac.0c00797.
[7] J. Cheng, T.J. Deming, Synthesis of polypeptides by ring-opening polymerization of α-amino acid N-carboxyanhydrides, Top. Curr. Chem. 310 (2012) 1–26, https://doi.org/10.1007/128_2011_173.
[8] Y. Ma, Y. Shen, Z. Li, Different cell behaviors induced by stereochemistry on polypeptide brush grafted surfaces, Mater. Chem. Front. 1 (2017) 846–857, https://doi.org/10.1039/c6qm00200e.
[9] P. Nair, G.R. Navale, M.S. Dharne, Poly-gamma-glutamic acid biopolymer: a sleeping giant with diverse applications and unique opportunities for commercialization, Biomass Convers. Biorefin. 1 (2021) 1–19, https://doi.org/10.1007/s13399-021-01467-0.
[10] Y. Fang, X. Zhu, N. Wang, X. Zhang, D. Yang, J. Nie, G. Ma, Biodegradable core-shell electrospun nanofibers based on PLA and γ-PGA for wound healing, Eur. Polym. J. 116 (2019) 30–37, https://doi.org/10.1016/j.eurpolymj.2019.03.050.
[11] J. Qian, X. Yong, W. Xu, X. Jin, Preparation and characterization of bimodal porous poly(γ-benzyl-L-glutamate) scaffolds for bone tissue engineering, Mater. Sci. Eng. C 33 (2013) 4587–4593, https://doi.org/10.1016/j.msec.2013.07.016.
[12] J. Han, J. Ding, Z. Wang, S. Yan, X. Zhunag, X. Chen, J. Yin, The synthesis, deprotection and properties of poly(γ-benzyl-L-glutamate), Sci. China Chem. 56 (2013) 729–738, https://doi.org/10.1007/s11426-013-4839-3.
[13] M. Song, S.P. Yu, O. Mohamad, W. Cao, Z.Z. Wei, X. Gu, M.Q. Jiang, L. Wei, Optogenetic stimulation of glutamatergic neuronal activity in the striatum enhances neurogenesis in the subventricular zone of normal and stroke mice, Neurobiol. Dis. 98 (2017) 9–24, https://doi.org/10.1016/j.nbd.2016.11.005.
[14] T.C. Chen, P.Y. She, D.F. Chen, J.H. Lu, C.H. Yang, D.S. Huang, P.Y. Chen, C.Y. Lu, K.S. Cho, H.F. Chen, W.F. Su, Polybenzyl glutamate biocompatible scaffold promotes the efficiency of retinal differentiation toward retinal ganglion cell lineage from human-induced pluripotent stem cells, Int. J. Mol. Sci. 20 (2019) 178, https://doi.org/10.3390/ijms20010178.
[15] C.Y. Lin, S.C. Luo, J.S. Yu, T.C. Chen, W.F. Su, Peptide-based polyelectrolyte promotes directional and long neurite outgrowth, ACS Appl. Bio Mater. 2 (2019) 518–526, https://doi.org/10.1021/acsabm.8b00697.
[16] M. Zheng, M. Pan, W. Zhang, H. Lin, S. Wu, C. Lu, S. Tang, D. Liu, Poly(α-L-lysine)-based nanomaterials for versatile biomedical applications: current advances and perspectives, J. Cai, Bioact. Mater. 6 (2021) 1878–1909, https://doi.org/10.1016/j.bioactmat.2020.12.001.
[17] N. Ardjomandi, C. Klein, K. Kohler, A. Maurer, H. Kalbacher, J. Niederländer, D. Alexander, Indirect coating of RGD peptides using a poly-L-lysine spacer enhances jaw periosteal cell adhesion, proliferation, and differentiation into osteogenic tissue, J. Biomed. Mater. Res. Part A. 100 (2012) 2034–2044, https://doi.org/10.1002/jbm.a.34062.
[18] A. Sharma, A. Goring, K.A. Staines, R.J.H. Emery, A.A. Pitsillides, R.O.C. Oreffo, S. Mahajan, C.E. Clarkin, Raman spectroscopy links differentiating osteoblast matrix signatures to pro-angiogenic potential, Matrix Biol. Plus. 5 (2019) 100018, https://doi.org/10.1016/j.mbplus.2019.100018.
[19] A. Orlowska, P.T. Perera, M.A. Kobaisi, A. Dias, H.K.D. Nguyen, S. Ghanaati, V. Baulin, R.J. Crawford, E.P. Ivanova, The effect of coatings and nerve growth factor on attachment and differentiation of pheochromocytoma cells, Mater. 11 (2017) 60, https://doi.org/10.3390/ma11010060.
[20] Z.H. Wang, Y.Y. Chang, J.G. Wu, C.Y. Lin, H.L. An, S.C. Luo, T.K. Tang, W.F. Su, Novel 3D neuron regeneration scaffolds based on synthetic polypeptide containing neuron cue, Macromol. Biosci. 18 (2018) 1700251, https://doi.org/10.1002/mabi.201700251.
[21] J.J. Medina Benavente, H. Mogami, T. Sakurai, K. Sawada, Evaluation of silicon nitride as a substrate for culture of PC12 cells: an interfacial model for functional studies in neurons, PLoS One 9 (2014), e90189, https://doi.org/10.1371/journal.pone.0090189.
[22] M. Rodriguez Sala, K.J. Lynch, S. Chandrasekaran, O. Skalli, M. Worsley, F. Sabri, PC-12 cells adhesion and differentiation on carbon aerogel scaffolds, MRS Commun. 8 (2018) 1426–1432, https://doi.org/10.1557/mrc.2018.206.
[23] B. Wiatrak, A. Kubis-Kubiak, A. Piwowar, E. Barg, PC12 cell line: cell types, coating of culture vessels, differentiation and other culture conditions, Cells. 9 (2020) 958, https://doi.org/10.3390/cells9040958.
[24] L.D. Riccardis, A. Ferramosca, A. Danieli, G. Trianni, V. Zara, F.D. Robertis, M. Maffia, Metabolic response to glatiramer acetate therapy in multiple sclerosis patients, BBA Clin. 6 (2016) 131–137, https://doi.org/10.1016/j.bbacli.2016.10.004.
[25] V. Dmitrovic, G.J.M. Habraken, M.M.R.M. Hendrix, W.J.E.M. Habraken, A. Heise, G. De With, N.A.J.M. Sommerdijk, Random poly (amino acid) s synthesized by ring opening polymerization as additives in the biomimetic mineralization of $CaCO_3$, Polymers. 4 (2012) 1195–1210, https://doi.org/10.3390/polym4021195.
[26] H. Zheng, T. Yoshitomi, K. Yoshimoto, Analysis of chirality effects on stem cell fate using three-dimensional fibrous peptide hydrogels, ACS Appl. Bio. Mater. 1 (2018) 538–543, https://doi.org/10.1021/acsabm.8b00123.
[27] W.H. Lang, G. Calloni, R.M. Vabulas, Polylysine is a proteostasis network-engaging structural determinant, J. Proteome Res. 17 (2018) 1967–1977, https://doi.org/10.1021/acs.jproteome.8b00108.
[28] G. Liu, D. Zhang, C. Feng, Control of three-dimensional cell adhesion by the chirality of nanofibers in hydrogels, Angew. Chem. Int. Ed. 53 (2014) 7789–7793, https://doi.org/10.1002/anie.201403249.
[29] Y. Liu, X. Wu, X. Sun, D. Wang, Y. Zhong, D. Jiang, T. Wang, D. Yu, N. Zhang, Design, synthesis, and evaluation of VEGFR-targeted macromolecular MRI contrast agent based on biotin-avidin-specific binding, Int. J. Nanomedicine 12 (2017) 5039–5052, https://doi.org/10.2147/IJN.S131878.
[30] B. Li, Y. Wu, W. Zhang, S. Zhang, N. Shao, W. Zhang, L. Zhang, J. Fei, Y. Dai, R. Liu, Efficient synthesis of amino acid polymers for protein stabilization, Biomater. Sci. 7 (2019) 3675–3682, https://doi.org/10.1039/C9BM00484J.
[31] N. Hann, Effects of lithium bromide on the gel-permeation chromatography of polyester-based polyurethanes in dimethylformamide, J. Polym. Sci. 15 (1977) 1331–1339, https://doi.org/10.1002/pol.1977.170150604.
[32] W.F. Su, Principles of polymer design and synthesis, Springer 3 (4) (2013) 27–87, https://doi.org/10.1007/978-3-642-38730-2.
[33] Prakash R. Sultane, Trimbak B. Mete, Ramakrishna G. Bhat, A convenient protocol for the deprotection of N-benzyloxycarbonyl (Cbz) and benzyl ester groups, Tetrahedron Lett. 56 (2015) 2067–2070, https://doi.org/10.1016/j.tetlet.2015.02.131.
[34] H.S. Mansur, C.M. Sadahira, A.N. Souza, A.A.P. Mansur, FTIR spectroscopy characterization of poly (vinyl alcohol) hydrogel with different hydrolysis degree and chemically crosslinked with glutaraldehyde, Mater. Sci. Eng. C 28 (2008) 539–548, https://doi.org/10.1016/j.msec.2007.10.088.
[35] P. Maria, P. Roberto, FTIR analysis of hydrolysis in aliphatic polyesters, Polym. Degrad. Stab. 92 (2007) 1491–1497, https://doi.org/10.1016/j.polymdegradstab.2007.05.009.